I&EC research
Industrial & Engineering Chemistry Research

Article

pubs.acs.org/IECR

# Influence of Aminosilane Coupling Agent on Aromatic Polyamide/Intercalated Clay Nanocomposites

Muhammad Usman Alvi,[†] Sonia Zulfiqar,*[,‡] Cafer T. Yavuz,[§] Hee-Seok Kweon,[∥] and Muhammad Ilyas Sarwar*[,†]

[†]Department of Chemistry, Quaid-i-Azam University, Islamabad 45320, Pakistan

[‡]Department of Physics, COMSATS Institute of Information Technology, Islamabad 44000, Pakistan

[§]Graduate School of EEWS, Korea Advanced Institute of Science and Technology, 335 Gwahangno, Yuseong-gu, Daejeon 305-701, Republic of Korea

[∥]Division of Electron Microscopic Research, Korea Basic Science Institute, 169-148 Gwahangno, Yuseong-gu, Daejeon 305-806, Republic of Korea



**ABSTRACT:** Aminosilane grafted and diamine modified reactive montmorillonite was exploited to generate aromatic polyamide based nanocomposites. For better compatibility, the hydrophilic nature of montmorillonite was changed into organophilic using 1,4-phenylenediamine, and the hydroxyl groups present on the clay surface and edges were used to graft 3-aminopropyltriethoxysilane (APTS) on clay sheets. The dispersion of clay was monitored in the polyamide obtained from 1,4-phenylenediamine, 4,4′-oxydianiline, and isophthaloyl chloride. These chains were converted into carbonyl chloride ends to interact with free amine groups of grafted APTS and diamine. Thin films were probed for FTIR, XRD, SEM, TEM, tensile testing, TGA, and DSC measurements. The results described ample dispersion of clay in the nanocomposites with tensile strength increased 110% and elongation increased 172% upon the addition of 4−6 wt % clay. Thermal decomposition temperatures of the nanocomposites were in the range 425−480 °C. The glass transition temperature increased up to 142.4 °C with 6 wt % addition of organoclay.

## 1. INTRODUCTION

Nanocomposites have become state of the art as structural materials in the field of engineering because of their improved mechanical, thermal, barrier, and fire retardant properties.[1−3] The properties of such materials depend on various factors such as nature, properties, content, dimensions, and microstructure of reinforcement.[4] Nanocomposite properties are influenced by interfacial interactions between the matrix and the dispersed phase. The aspect ratio of the clay is also very vital and crucial in nanocomposites for electrical,[5,6] mechanical,[7] thermal,[8−11] and barrier properties.[12,13] Nanocomposites based on layered silicates, carbon nanotubes, and nanofibers are receiving considerable attention due to low density along with ease of processability, and their unique multifunctional and highly enhanced properties[14−16] relative to those of conventional microcomposites.

Clay nanocomposites typically exhibit superior properties provided the silicate layers are homogenously dispersed throughout the matrix at nanoscale.[17−25] The uniform dispersion of silicate layers is usually desirable for maximum reinforcement of the materials. The lack of interfacial interactions between the hydrophilic layered silicates and the hydrophobic polymer matrix does not allow the individual nanolayers to be easily separated and dispersed in the polymers. This interfacial problem can be solved, at least in part, either by functionalizing the clay platelets, by adding a swelling agent, or by doing both to obtain organically modified clay prior to use in nanocomposite formation. Silane functionalized montmorillonite (MMT) and its influence on the properties of water based polymer/clay nanocomposites have been investigated.[26] Epoxy nanocomposites with pristine MMT, organically modified montmorillonite (OMMT), and aminosilane functionalized MMT have been prepared and characterized for mechanical and dynamic mechanical analyses. Comparison of these resulting materials clearly indicated the influence of chemical interaction between aminosilane functionalized MMT and epoxy on the composite properties.[27] The structural, morphological, and mechanical properties of polyethylene (PE)−clay nanocomposites using an aminosilane modified polyethylene (PE-*g*-AS) as a compatibilizer have been studied. The PE-*g*-AS was obtained by condensation reaction between the amine group of 3-aminopropyltriethoxysilane (APTS) and the maleic anhydride moiety of PE-*g*-MA. The triethoxysilyl group reacted with the hydroxyl group on the clay surface to form a linkage between polymer and clay, thus increasing the interaction and dispersion of the clay in the matrix. Although an aminosilane modified polypropylene (PP-*g*-AS) was used as compatibilizer for PP−clay nanocomposites,[28] aminosilane polyethylene (PE-*g*-AS) was used as a compatibilizer in a PE/organoclay nanocomposite system.[29] Some other related studies described the incorporation of silane-coupling agents in the preparation of polymer−clay nanocomposites for increasing the organic−inorganic interactions.[30,31]

**Received:** February 10, 2013
**Revised:** April 21, 2013
**Accepted:** April 30, 2013
**Published:** April 30, 2013

   dx.doi.org/10.1021/ie400463z | *Ind. Eng. Chem. Res.* 2013, 52, 6908−6915

**Scheme 1. Formation of Aromatic Polyamide Matrix with COCl End Groups**

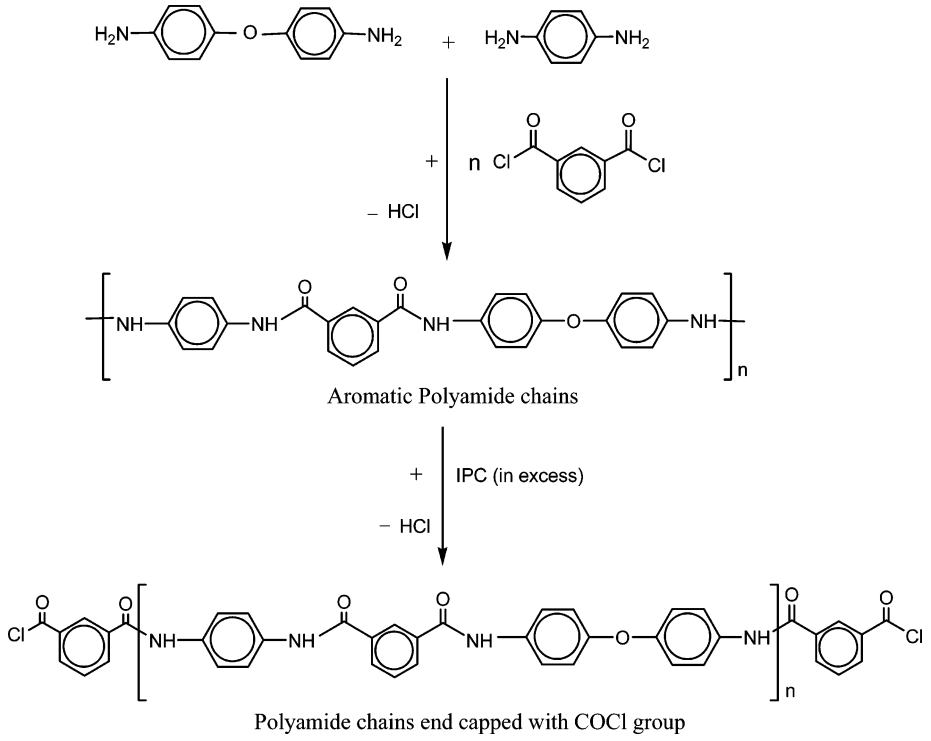


Aromatic polyamides are the most important class of high performance polymers, because they have superb mechanical profiles, thermal stability, chemical resistance, and low flammability and are good substitutes for ceramics and metals in the automotive, aerospace, and microelectronics industries. Moreover, chain stiffness and intermolecular hydrogen bonding between amide groups limit their solubility in organic solvents and render high glass transition or melting temperatures, making their processability difficult. Modification in the backbone of these polymers with flexible linkages generally increased the solubility[32−34] and lowered the glass transition temperatures without sacrificing the thermal stability.[35] Copolyamides containing aryl ether or aryl sulfone or meta-linkages possess lower glass transition temperatures, greater chain flexibility, and greater tractability than their corresponding analogues without these groups in the backbone. Different hybrid materials based on soluble aromatic polyamides have already been reported.[36−38]

In this study, aromatic polyamides with enhanced solubilities in organic solvents were synthesized by condensing a pair of diamines, 1,4-phenylenediamine and 4,4′-oxydianiline, with isophthaloyl chloride in anhydrous dimethylacetamide (DMAc). These polymer chains were purposely converted into carbonyl chloride end groups using excess diacid chloride near the end of the polymerization reaction. For homogeneous dispersion of clay into the polyamide matrix, first its nature was changed from hydrophilic to organophilic by inserting the cationic form of 1,4-phenylenediamine between clay layers. Then a reaction was carried out between intercalated clay and 3-aminopropyltriethoxysilane in the water/ethanol system. The triethoxysilane groups of APTS condensed with hydroxyl groups present on surfaces and edges of the clay, whereas free amino groups of APTS and swelling agent were used to react with reactive carbonyl chloride chain ends of the polyamide matrix. In this way, the intercalating effect became strong and more permanent because a massive amount of polyamide chains chemically connected to the swelling and coupling agents, producing thermally stable and mechanically robust nanocomposites. To the best of our knowledge, this is the first report on the preparation of aromatic polyamide and aminosilane functionalized OMMT nanocomposites. Thin nanocomposite films with different clay loadings were prepared and characterized using various techniques to examine the morphology, mechanical properties, and thermal properties.

## 2. MATERIAL AND METHODS

**2.1. Materials.** Various monomers such as 1,4-phenylenediamine, 4,4′-oxydianiline, and isophthaloyl chloride and other chemicals including triethylamine, ethanol, and hydrochloric acid were obtained from Fluka and used as received. *N*,*N*-Dimethylacetamide, montmorillonite (MMT), 3-aminopropyltriethoxysilane, and silver nitrate were obtained from Aldrich and used as received.

**2.2. Synthesis of Aromatic Polyamide.** The polymerization of monomers was carried out by placing a mixture of 1,4-phenylenediamine and 4,4′-oxydianiline in the flask along with DMAc as a solvent under an inert atmosphere. After 15 min, a stoichiometric amount of isophthaloyl chloride was added to the diamine mixture under anhydrous conditions. The contents of the flask were cooled below 0 °C to avoid any side reaction due to the exothermic nature of the reaction. Then the reaction was allowed to come to ambient temperature after 1 h. In order to create interactions between aromatic polyamide and the clay, the polymer chains were end-capped with carbonyl chloride groups using a slight excess of isophthaloyl chloride at a later stage. Although the reaction between diamines and diacid chloride is very fast, the flask was agitated for an additional 24 h to ensure its completion.[28] A stoichiometric amount of triethylamine was added to quench HCl formed as precipitate. The polyamide resin separated from the precipitate


dx.doi.org/10.1021/ie400463z | Ind. Eng. Chem. Res. 2013, 52, 6908−6915

by centrifugation was golden yellow in color. The formation of carbonyl chloride end-capped aromatic polyamide chains is shown in Scheme 1.

**2.3. Modification of MMT.** The intercalation or modification of MMT was done by an ion exchange method in aqueous medium. In a typical intercalation procedure, 1,4-phenylenediamine was placed in a beaker containing water, followed by the addition of a stoichiometric amount of concentrated hydrochloric acid. The solution was heated at 80 °C. In a separate beaker, MMT was dispersed in water at 80 °C and was added to a solution of ammonium salt of 1,4-phenylenediamine with vigorous stirring for 3 h at 60 °C. The precipitates were isolated by filtration and washed with hot water with stirring for 1 h and then filtered. This process was repeated three times to remove the residual amount of swelling agent. The filtrate was titrated with $AgNO_3$ until there were no AgCl precipitates to ensure the complete removal of chloride ions. The final product obtained by filtration was dried in a vacuum oven at 60 °C for 24 h. The dried cake was ground to a fine powder. The formation of organoclay (OMMT) is given in Scheme 2.

**Scheme 2. Intercalation or Organic Modification of MMT**

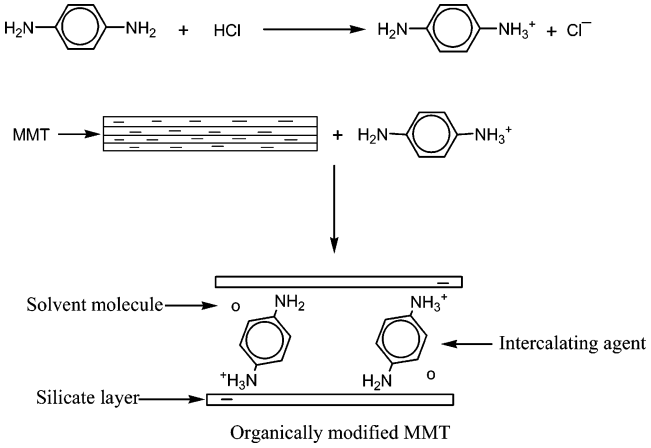


**2.4. Silane Functionalization of OMMT.** Silane functionalization of OMMT was carried out in a mixture of the ethanol/water system. OMMT (2.5 g) was added in a flask, provided with stirring followed by addition of an ethanol/water solution 75/25 by volume. After complete dispersion of OMMT, 3-aminopropyltriethoxysilane (2.0 g) was introduced into the above mixture and agitated for 8 h at 80 °C. The resultant product was washed using a mixture of ethanol/water 8−12 times in order to remove the residual silane and dried at 60 °C in a vacuum oven and used for the formation of nanocomposites. The formation of aminosilane functionalized OMMT is given in Scheme 3.

**2.5. Formation of Nanocomposite Films.** Nanocomposite films were prepared by mixing a measured amount of polyamide solution with a known quantity of modified clay in a flask for a desired concentration. For homogeneous dispersion of nanoclay in the polymer matrix, the mixture was kept at a constant high speed stirring at room temperature for 24 h. Similarly other concentrations (2−10 wt %) of the nanocomposites were prepared by mixing different amounts of clay with the polyamide solution. Hybrid films of uniform thickness were obtained by pouring the above prepared reaction mixtures into Petri dishes and evaporating the solvent at high

**Scheme 3. Silane Functionalization of Intercalated Montmorillonite (OMMT)**

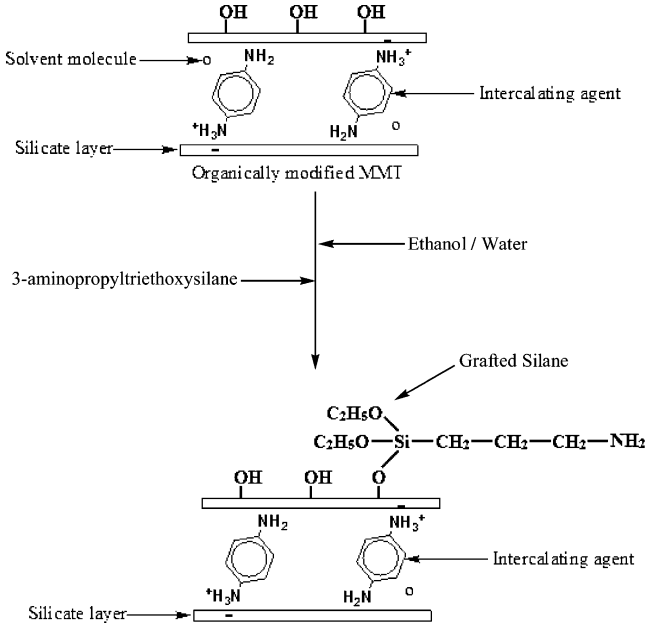


temperature. Films were further dried at 60 °C under vacuum to a constant weight. The flow sheet for the preparation of nanocomposites is illustrated in Scheme 4.

**2.6. Characterization.** The structural determinations of the matrix, neat MMT, modified MMT, and thin nanocomposite films were carried out using an Excalibur series Thermo Nicolet 6700 FTIR spectrophotometer, over the range 4000−500 $cm^{-1}$. The diffraction pattern was recorded using an X-ray diffractometer 3040/60 X'Pert PRO PANalytical in reflection mode (radiation wavelength = 0.154 nm). The scanning angle for these measurements was kept between $2\theta = 2°$ and $2\theta = 40°$, with a step size of 0.02°. The surface morphology of synthesized nanocomposite films was monitored with an FEI Nova 230 field emission scanning electron microscope, whereas the internal morphology of ultramicrotomed samples was observed by an FEI Tecnai G2 Spirit Twin transmission electron microscope, operated at an accelerating voltage of 120 kV. Tensile properties of the nanocomposites (rectangular strips) having dimensions ca. 14 mm × 5.0−6.9 mm × 0.19−0.37 mm were measured according to DIN Procedure 53455 having a crosshead speed of 5 mm $min^{-1}$ at 25 °C using a Testometric Universal Testing Machine M500-30, and an average value obtained from five to seven different measurements in each case has been reported. The thermal stabilities of the nanocomposites were determined using a METTLER TOLEDO TGA/SDTA 851$^e$ thermogravimetric analyzer using 1−5 mg of the sample in an $Al_2O_3$ crucible heated from 25 to 900 °C at a heating rate of 10 °C $min^{-1}$ under nitrogen atmosphere with a gas flow rate of 30 mL $min^{-1}$. Thermomechanical properties of these materials were measured using a METTLER TOLEDO DSC 822$^e$ differential scanning calorimeter. For determining the glass transition temperatures, samples of 5−10 mg were encapsulated in aluminum pans and heated at a ramp rate of 10 °C $min^{-1}$ under nitrogen atmosphere.


dx.doi.org/10.1021/ie400463z | Ind. Eng. Chem. Res. 2013, 52, 6908−6915

**Scheme 4. Formation of Polyamide/Silane Functionalized OMMT Nanocomposites**

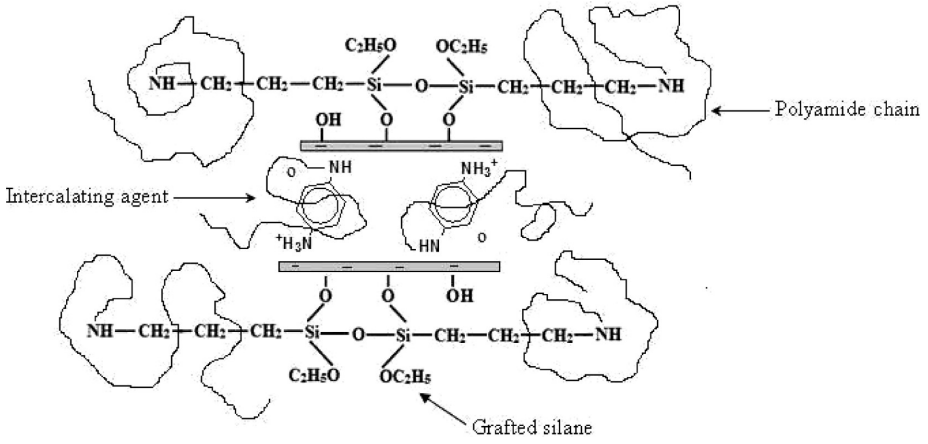


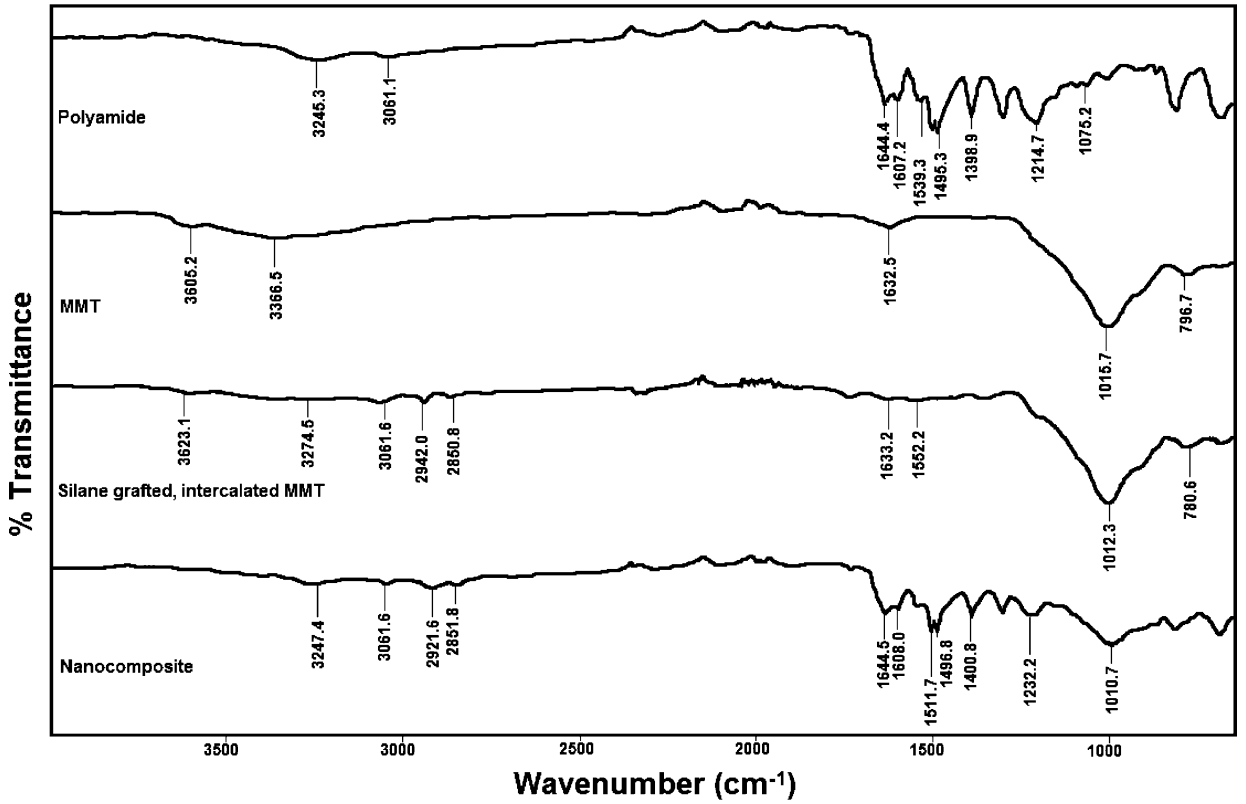


**Figure 1.** FTIR spectra of pure polyamide, MMT, silane functionalized OMMT, and nanocomposite film.

## 3. RESULTS AND DISCUSSION

The chemical structures of the polyamide matrix, MMT, silane grafted OMMT, and nanocomposites were determined by IR spectroscopy. The thin film obtained from pure polyamide resin was transparent and golden yellow in color. This color changed to black upon the addition of silane grafted OMMT. The transparency of the composite films decreased by the addition of clay, and the films became semitransparent as well as brittle at high loading of clay. Different analyses carried out for the characterization of these materials are described below.

**3.1. Fourier Transform Infrared (FTIR) Spectroscopy.** The IR spectra of pure polyamide matrix, neat MMT, silane grafted OMMT, and nanocomposite films were monitored, and the related data are represented in Figure 1. Various bands of aromatic polyamide appeared for N−H stretching and bending at 3245 and 1607 $cm^{-1}$, aromatic C−H stretching at 3061 $cm^{-1}$, aromatic C═C stretching at 1539 and 1495 $cm^{-1}$, and C−O—C asymmetric and symmetric stretching at 1214 and 1075 $cm^{-1}$, respectively. A band for C═O stretching was scrutinized at 1644 $cm^{-1}$ and broadening of the band denoted C═O was seen in both free and combined environments. Pristine MMT gave an intense band at 1015 $cm^{-1}$ for Si−O stretch and bands for O−H group stretching and bending vibrations at 3625 and 796 $cm^{-1}$, confirming the presence of hydroxyl groups on the surface of silicate layers. The stretching and bending absorption of water molecules adsorbed on clay appeared at 3366 and 1632 $cm^{-1}$. In silane grafted OMMT, two additional bands at 3061 and 1552 $cm^{-1}$ illustrated the aromatic C−H stretching and N−H bending of aromatic diamine (swelling agent), confirming the intercalation of clay with


dx.doi.org/10.1021/ie400463z | Ind. Eng. Chem. Res. 2013, 52, 6908−6915

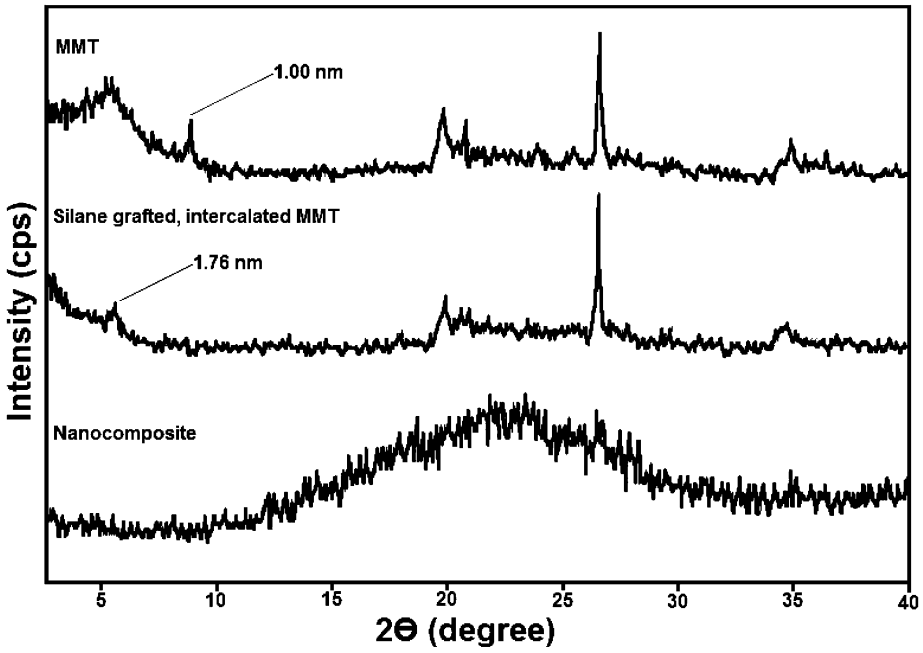


**Figure 2.** XRD patterns of neat MMT, silane functionalized OMMT, and nanocomposite film.

aromatic diamine. Two closely related bands at 2942 and 2850 $cm^{-1}$ represented the asymmetric and symmetric stretching of $CH_2$ groups of APTS. The stretching vibration of O−H groups attached on clay was observed at 3623 $cm^{-1}$ with decreased intensity relative to the untreated clay, and the bending vibration of O−H groups appeared at 780 $cm^{-1}$. These bands confirmed the successful grafting of silane with intercalated clay. The spectrum of nanocomposite film showed characteristic bands of silane grafted OMMT and polyamide. The bands of the pure matrix appeared for N−H stretching and bending at 3245 and 1607 $cm^{-1}$, aromatic C−H stretching at 3061 $cm^{-1}$, aromatic C═C stretching at 1539 and 1495 $cm^{-1}$, C═O stretching at 1644 $cm^{-1}$, and C−O−C asymmetric and symmetric stretching at 1214 and 1075 $cm^{-1}$ respectively. The asymmetric and symmetric stretching of $CH_2$ groups of grafted silane were represented at 2921 and 2851 $cm^{-1}$ with Si−O stretching at 1010 $cm^{-1}$ assigned to silicate layers of clay.

**3.2. X-ray Diffraction (XRD) Analysis.** The distribution of clay in the nanocomposites was obtained by comparing XRD patterns of neat MMT, silane grafted OMMT, and nanocomposites as given in Figure 2. MMT gave a $d$-spacing of 1.0 nm around $2\theta$ = 8.82°, while silane grafted OMMT demonstrated a shift toward a lower angle ($2\theta$ = 5.0°), giving a larger $d$-spacing ($d$ = 1.760 nm). This shifting of the (001) reflection toward a lower angle indicated successful modification of MMT because of the replacement of small $Na^+$ ions with large cationic aromatic diamine and grafting of silane with hydroxyl groups of clay. The nanocomposite pattern presented no peak in the low $2\theta$ angle, verifying ample distribution of clay in the matrix. No sharp peak characteristic of clay appeared due to insertion of polyamide chains in the interlayers of clay disrupting the ordered structures. These results led to the exfoliated/intercalated dispersion of silane grafted OMMT in the polyamide matrix. The increased interactions allowed the polymer chains to move into the interlayer spaces of clay for a uniform dispersion and greater interfacial bonding between the phases. However, XRD results provide incomplete information about the extent of nanolayer dispersion and some additional information is required in order to confirm homogeneous clay dispersion.

**3.3. Morphological Analysis.** XRD studies gave some but not complete information about the level of dispersion including no peak representing delaminated clay. For this reason, further investigation of the nanostructure was carried out by field emission scanning electron microscopy (FESEM) and transmission electron microscopy (TEM). Investigations of the surface morphologies of nanocomposites with 2 and 6 wt % clay were carried out on the fractured surfaces of thin films, and FESEM images are shown in Figure 3. Micrographs presented a network on the surfaces of the nanocomposites with an ample

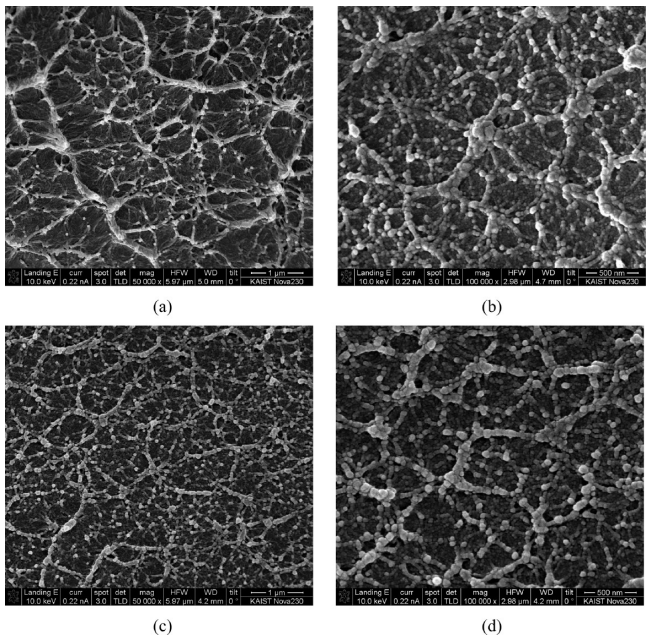


**Figure 3.** FESEM micrographs of polyamide/silane functionalized OMMT nanocomposites: (a and b) 2 wt % clay; (c and d) 6 wt % clay.


dx.doi.org/10.1021/ie400463z | Ind. Eng. Chem. Res. 2013, 52, 6908−6915

distribution in the matrix. Interconnected domains in micrographs demonstrated good compatibility between the two disparate phases. The idea of modifying the nature of clay from hydrophilic to organophilic through swelling and coupling agents provided better interfacial interactions. The dispersion of clay layers can be seen more clearly by viewing TEM micrographs as shown in Figure 4. The polyamide with 2 wt

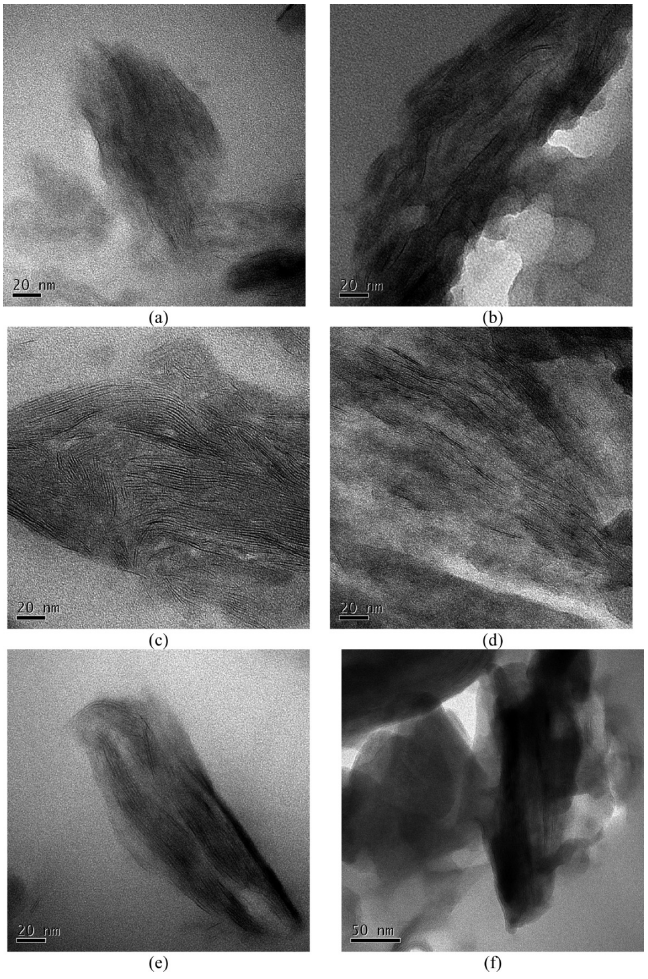


**Figure 4.** TEM images of polyamide/silane functionalized OMMT nanocomposites: (a and b) 2 wt % at 220000×; (c and d) 6 wt % at 220000×; (e and f) 10 wt % clay at (e) 220000× and (f) 150000×, respectively.

% clay content in the matrix revealed a fine dispersion of silane grafted OMMT, suggesting that silicate layers exfoliated in polyamide matrix and nanocomposites were formed (Figure 4a,b). At a higher percentage of silane grafted OMMT (6 wt %) in nanomaterials, individual clay platelets were predominant with some tactoids indicating that the morphology was partially exfoliated and partially intercalated (Figure 4c,d). At 10 wt % clay content, more agglomerated clay platelets were visible in the micrographs (Figure 4e,f). However, the dimensions of these stacks are too small to give any diffraction peak in the XRD pattern. These results are in complete agreement with results of XRD analysis.

**3.4. Tensile Testing.** Mechanical properties of the materials indicate how the material would respond to forces being applied in tension. Stress–strain curves and other mechanical properties of nanocomposites measured with different concentrations of silane grafted OMMT are given in Figure 5 and Table 1. The modulus of the nanocomposites

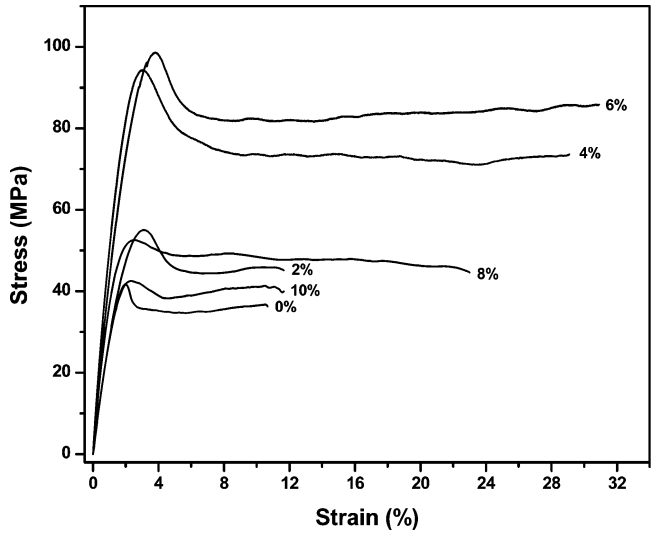


**Figure 5.** Stress–strain curves of polyamide/silane functionalized OMMT nanocomposites.

**Table 1. Mechanical Data of Polyamide/Silane Functionalized OMMT Nanocomposites**

| clay loading (%) | max stress ± 1.0 (MPa) | max strain ± 0.02 (%) | toughness ± 0.2 (×10$^6$ J m$^{-3}$) | tensile modulus ± 0.02 (GPa) |
|---|---|---|---|---|
| 0 | 42 | 11 | 361 | 2.54 |
| 2 | 55 | 12 | 507 | 2.96 |
| 4 | 94 | 29 | 2128 | 4.55 |
| 6 | 98 | 30 | 2523 | 4.05 |
| 8 | 53 | 20 | 1076 | 3.10 |
| 10 | 44 | 12 | 439 | 2.45 |

increased from 2.54 GPa for pure polyamide to a maximum value 4.55 GPa with 4 wt % layered silicate, beyond which it decreased. The maximum stress for the pure polymer was 42 MPa; that increased to 98 MPa with 6 wt % clay and then it decreased with increase in clay content. The length at break and toughness of these materials increased up to 6 wt % clay content in the matrix. Tensile data revealed improvements in the mechanical properties of the nanocomposites relative to pristine polyamide matrix due to the interfacial interactions between the two phases. Intercalation and functionalization of MMT with 1,4-phenylenediamine and 3-aminopropyltriethoxysilane on one hand interacted with clay while free amine groups on the other hand reacted with carbonyl chloride groups of the polyamide. These interactions solved the stress transfer problem efficiently between the matrix and reinforcement, producing mechanically robust nanocomposites. However, this improvement in properties was limited only to low concentrations of reinforcement, because at high concentrations phase separation may take place which results in poor interfacial interactions between the two disparate phases, leading to brittleness and reduction in mechanical properties.

**3.5. Thermogravimetric Analysis.** The thermal stability of the polyamide/silane grafted OMMT nanocomposites monitored by thermogravimetric analysis is presented in Figure 6. Thermograms of nanocomposites were obtained in the temperature range 25–900 °C. Thermal decomposition


dx.doi.org/10.1021/ie400463z | Ind. Eng. Chem. Res. 2013, 52, 6908–6915

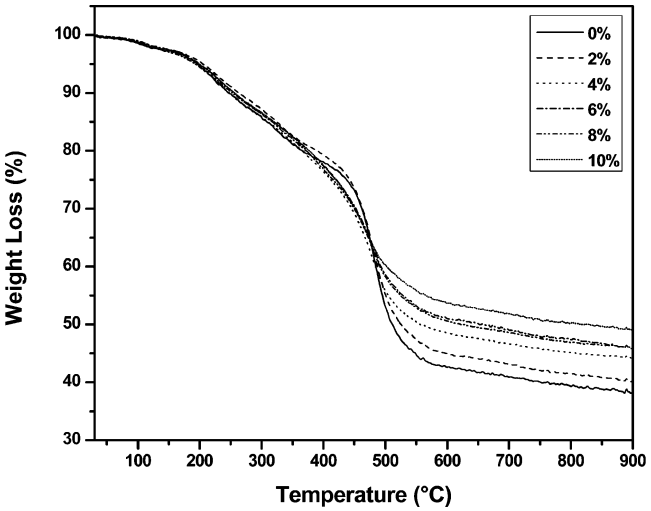


**Figure 6.** TGA curves of polyamide/silane functionalized OMMT nanocomposites.

temperatures of pure polyamide and hybrid materials were generally in the range 425−480 °C, and the thermal stability slightly increased with increase in clay concentration. The modification of clay was responsible for not only interactions between matrix and reinforcement but also increased delamination of nanolayers, thus improving the thermal profile of the nanocomposites. The weights of residues left after the decomposition at 900 °C were found to be approximately proportional to the clay content in the hybrids.

**3.6. Glass Transition Temperature.** The glass transition temperatures ($T_g$'s) of polyamide−clay nanocomposites were measured by differential scanning calorimetry (DSC), and the thermograms are presented in Figure 7. The $T_g$ of nano-

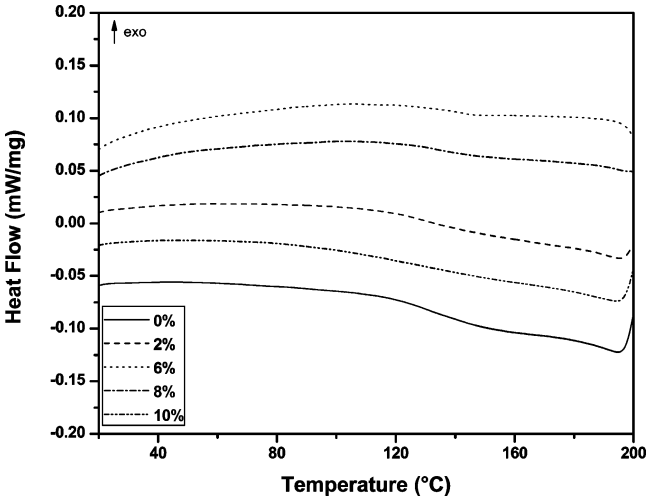


**Figure 7.** DSC thermograms of polyamide/silane functionalized OMMT nanocomposites.

composites increased relative to neat polyamide, showing an optimal increase in the $T_g$ value (142.4 °C) with 6 wt % addition of clay, and then decreased slightly with higher clay content. These results described a systematic increase in the $T_g$ values with increasing nanoclay content, indicating a greater interaction of the two disparate phases. Nanoclay reduced the segmental motion of the polymer chains and with increasing proportion of the inorganic phase shifted the baseline of the DSC curve toward higher temperature. This implied that polyamide chains chemically linked with silane modified silicate layers. As a result, the motion of polymer chain was restricted, thereby increasing the $T_g$ values of the composite materials. The $T_g$ values increased relative to pure polyamide due to the intercalation of the polymer chains into the interlayer of clay, which suppresses the mobility of polymer segments near the interface.

## 4. CONCLUSIONS

Aromatic polyamide/silane grafted OMMT nanocomposites were successfully prepared by a solution intercalation method. The incorporation of the silane grafted OMMT reinforced the polyamide matrix, depicting good compatibility between the two phases. The interfacial interactions through the carbonyl chloride of the polyamide and amine groups of the intercalating and coupling agents grafted on clay promoted strong interphase bonding between the two phases, resulting in enhanced thermomechanical properties of the nanocomposites. The dispersion of individual silicate sheets was optimum at low clay concentration, giving an observed increase in the mechanical properties of these materials. At high clay loading, it might exist in the form of agglomerates with lesser cohesion with the organic matrix and caused adverse effects on the mechanical properties. The thermal stabilities of hybrid materials were also increased by a corresponding increase in silane grafted OMMT content in the polyamide matrix.

## AUTHOR INFORMATION

### Corresponding Author

*Tel.: 0092-51-90642132 (M.I.S.); 0092-301-5017753 (S.Z.). Fax: 0092-51-90642241 (M.I.S.); 0092-51-9247006 (S.Z.). E-mail: ilyassarwar@hotmail.com (M.I.S.); soniazulfiqar@yahoo.com (S.Z.).

### Notes

The authors declare no competing financial interest.

## ACKNOWLEDGMENTS

The authors are thankful to the Higher Education Commission of Pakistan (HEC) for the financial support provided through project research grant 20-23-ACAD (R) 03-410 and appreciate the cooperation of the Electron Microscopic Research Team, especially Hye-Jin Cho, Korea Basic Science Institute, Daejeon, Republic of Korea.

## REFERENCES

(1) Cosoli, P.; Scocchi, G.; Pricl, S.; Fermaglia, M. Many-Scale Molecular Simulation for ABS-MMT Nanocomposites. *Microporous Mesoporous Mater.* **2008**, *107*, 169.

(2) Ma, H.; Xu, Z.; Tong, L.; Gu, A.; Fang, Z. Studies of ABS-grafted-Maleic Anhydride/Clay Nanocomposites: Morphology, Thermal Stability and Flammability Properties. *Polym. Degrad. Stab.* **2006**, *91*, 2951.

(3) Pandey, J. K.; Reddy, K. R.; Kumar, A. P.; Singh, R. P. An Overview on the Degradability of Polymer Nanocomposites. *Polym. Degrad. Stab.* **2005**, *88*, 234.

(4) Zhang, Z.; Friedrich, K. Artificial Neural Network Applied to Polymer Composites: A Review. *Compos. Sci. Technol.* **2003**, *63*, 2029.

(5) Sheng, N.; Boyce, M. C.; Parks, D. M.; Rutledge, G. C.; Abes, J. I.; Cohen, R. E. Multiscale Micromechanical Modeling of Polymer/Clay Nanocomposites and the Effective Clay Particle. *Polymer* **2004**, *45*, 487.

(6) Al-Saleh, M. H.; Sundararaj, U. Processing-Microstructure-Property Relationship in Conductive Polymer Nanocomposites. *Polymer* **2010**, *51*, 2740.
(7) Groosiord, N.; Loos, J.; Laake, L. V.; Maugey, M.; Zakri, C.; Koning, C. E.; Hart, A. J. High-Conductivity Polymer Nanocomposites Obtained by Tailoring the Characteristics of Carbon Nanotube Fillers. *Adv. Funct. Mater.* **2008**, *18*, 3226.
(8) Sarfaraz, A.; Warsi, M. F.; Sarwar, M. I.; Ishaq, M. Improvement in Tensile Properties of PVC-Montmorillonite Nanocomposites through Controlled Uniaxial Stretching. *Bull. Mater. Sci.* **2012**, *35*, 539.
(9) Zulfiqar, S.; Ahmad, Z.; Sarwar, M. I. Probing the Properties of Nanocomposites Synthesized from Aramid and Surface Modified Clay. *Aust. J. Chem.* **2009**, *62*, 441.
(10) Zulfiqar, S.; Sarwar, M. I. Investigating the Structure-Property Relationship of Aromatic-Aliphatic Polyamide/Layered Silicate Hybrid Films. *Solid State Sci.* **2009**, *11*, 1246.
(11) Zulfiqar, S.; Ahmad, Z.; Ishaq, M.; Sarwar, M. I. Aromatic-Aliphatic Polyamide/ Montmorillonite Clay Nanocomposite Materials: Synthesis, Nanostructure and Properties. *Mater. Sci. Eng., A* **2009**, *525*, 30.
(12) Zulfiqar, S.; Sarwar, M. I. Synthesis and Characterization of Aromatic-Aliphatic Polyamide Nanocomposite Films Incorporating a Thermally Stable Organoclay. *Nanoscale Res. Lett.* **2009**, *4*, 391.
(13) Gorrasi, G.; Tortora, M.; Vittoria, V.; Pollet, E.; Lepoittevin, B.; Alexandre, M. Vapor Barrier Properties of Polycaprolactone Montmorillonite Nanocomposites: Effect of Clay Dispersion. *Polymer* **2003**, *44*, 2271.
(14) Messersmith, P. B.; Giannelis, E. P. Synthesis and Barrier Properties of Poly(ε-caprolactone)-Layered Silicate Nanocomposites. *J. Polym. Sci., Part A: Polym. Chem.* **1995**, *33*, 1047.
(15) Zulfiqar, S.; Rafique, M.; Shaukat, M. S.; Ishaq, M.; Sarwar, M. I. Influence of Clay Modification on the Properties of Aramid/Layered Silicate Nanocomposites. *Colloid Polym. Sci.* **2009**, *287*, 715.
(16) Vaia, R. A.; Giannelis, E. P. Polymer Melts Intercalation in Organically-Modified Layered Silicates: Model Predictions and Experiment. *Macromolecules* **1997**, *30*, 8000.
(17) Kawasumi, M.; Hasegawa, N.; Kato, M.; Usuki, A.; Okada, A. Preparation and Mechanical Properties of Polypropylene-Clay Hybrids. *Macromolecules* **1997**, *30*, 6333.
(18) Wang, M. S.; Pinnavaia, T. J. Clay-Polymer Nanocomposites Formed from Acidic Derivatives of Montmorillonite and an Epoxy Resin. *Chem. Mater.* **1994**, *6*, 468.
(19) Lan, T.; Kaviratna, P. D.; Pinnavaia, T. J. On the Nature of Polyimide-Clay Hybrid Composites. *Chem. Mater.* **1994**, *6*, 573.
(20) Fornes, T. D.; Yoon, P. J.; Hunter, D. L.; Keskkula, H.; Paul, D. R. Effect of Organoclay Structure on Nylon-6 Nanocomposite Morphology and Properties. *Polymer* **2002**, *43*, 5915.
(21) Zulfiqar, S.; Lieberwirth, I.; Ahmad, Z.; Sarwar, M. I. New Aramid Based Nanocomposites: Synthesis and Characterization. *Polym. Eng. Sci.* **2008**, *48*, 1624.
(22) Zulfiqar, S.; Lieberwirth, I.; Ahmad, Z.; Sarwar, M. I. Influence of Oligomerically Modified Reactive Montmorillonite on Thermal and Mechanical Properties of Aromatic Polyamide/Clay Nanocomposites. *Acta Mater.* **2008**, *56*, 4905.
(23) Huang, X.; Lewis, S.; Brittain, W. J.; Vaia, R. A. Synthesis of Polycarbonate-Layered Silicate Nanocomposites via Cyclic Oligomers. *Macromolecules* **2000**, *33*, 2000.
(24) Huang, J. C.; Zhu, Z. K.; Qian, X. F.; Sun, Y. Y. Poly(etherimide)/Montmorillonite Nanocomposites Prepared by Melt Intercalation: Morphology, Solvent Resistance Properties and Thermal Properties. *Polymer* **2001**, *42*, 873.
(25) Messersmith, P. B.; Giannelis, E. P. Synthesis and Characterization of Layered Silicate-Epoxy Nanocomposites. *Chem. Mater.* **1994**, *6*, 1719.
(26) Herrera, N. N.; Letoffe, J. M.; Putaux, J. L.; David, L.; Bourgeat-Lami, E. Aqueous Dispersions of Silane-Functionalized Laponite Clay Platelets. A First Step toward the Elaboration of Water-Based Polymer/Clay Nanocomposites. *Langmuir* **2004**, *20*, 1564.
(27) Choi, Y. Y.; Lee, S. H.; Ryu, S. H. Effect of Silane Functionalization of Montmorillonite on Epoxy/Montmorillonite Nanocomposite. *Polym. Bull.* **2009**, *63*, 47.
(28) Liaw, W. C.; Huang, P. C.; Chen, C. S.; Lo, C. L.; Chang, J. L. PP-g-MA/APTS Compound Coupling Compatibilizer in PP/Clay Hybrid Nanocomposite. *J. Appl. Polym. Sci.* **2008**, *109*, 1871.
(29) Sánchez-Valdes, S.; Méndez-Nonell, J.; Medellín-Rodríguez, F. J.; Ramírez-Vargas, E.; Martínez-Colunga, J. G.; Soto-Valdez, H.; Muñoz-Jiménez, L.; Neira-Velázquez, G. Effect of PE-g-MA/Amine Silane Compatibilizer on Clay Dispersion of Polyethylene-Clay Nanocomposites. *Polym. Bull.* **2009**, *63*, 921.
(30) Wang, L.; Sheng, J. Graft Polymerization and Characterization of Butyl Acrylate onto Silane-Modified Attapulgite. *J. Macromol. Sci., Part A: Pure Appl. Chem.* **2003**, *40*, 1135.
(31) Seckin, T.; Gultek, A.; Icduygu, M. G.; Onal, Y. Polymerization and Characterization of Acrylonitrile with Methacryloxypropyltrimethoxy-silane Grafted Bentonite Clay. *J. Appl. Polym. Sci.* **2002**, *84*, 164.
(32) Zulfiqar, S.; Ishaq, M.; Ahmad, Z.; Sarwar, M. I. Synthesis, Static and Dynamic Light Scattering Studies of Soluble Aromatic Polyamide. *Polym. Adv. Technol.* **2008**, *19*, 1250.
(33) Zulfiqar, S.; Lieberwirth, I.; Sarwar, M. I. Soluble Aramid Containing Ether Linkages: Synthesis, Static and Dynamic Light Scattering Studies. *Chem. Phys.* **2008**, *344*, 202.
(34) Zulfiqar, S.; Sarwar, M. I. Soluble Aromatic Polyamide Bearing Sulfone Linkages: Synthesis and Characterization. *High Perform. Polym.* **2009**, *21*, 3.
(35) Zulfiqar, S.; Ishaq, M.; Sarwar, M. I. Synthesis and Characterization of Soluble Aromatic-Aliphatic Polyamide. *Adv. Polym. Technol.* **2010**, *29*, 300.
(36) Sarwar, M. I.; Zulfiqar, S.; Ahmad, Z. Properties of Polyamide-Zirconia Nanocomposites Prepared from Sol-Gel Technique. *Polym. Compos.* **2009**, *30*, 95.
(37) Sarwar, M. I.; Zulfiqar, S.; Ahmad, Z. Investigating the Property Profile of Polyamide-Alumina Nanocomposite Materials. *Scr. Mater.* **2009**, *60*, 988.
(38) Zulfiqar, S.; Shabbir, S.; Ishaq, M.; Sarwar, M. I. Investigation of Nanostructure and Properties of Aromatic-Aliphatic Polyamide based Nanocomposites with Clay Additives. *J. Appl. Polym. Sci.* **2009**, *112*, 3141.